Sulbactam Forms Only Minimal Amounts of Irreversible Acrylate-Enzyme with SHV-1 β-Lactamase[†]

Monica A. Totir,[‡,§] Marion S. Helfand,[‡,‖,⊥] Marianne P. Carey,[‡] Anjaneyulu Sheri,[#] John D. Buynak,[#] Robert A. Bonomo,[‖,⊥,∇] and Paul R. Carey*,[‡,§]

Departments of Biochemistry, Chemistry, Medicine, and Pharmacology, Case Western Reserve University, Cleveland, Ohio 44106, Research Division, Louis Stokes Cleveland Veterans Affairs Medical Center, Cleveland, Ohio 44106, and Department of Chemistry, Southern Methodist University, Dallas, Texas 75205

ABSTRACT: Sulbactam is a mechanism-based inhibitor of β-lactamase enzymes used in clinical practice. It undergoes a complex series of chemical reactions in the active site that have been studied extensively in the past three decades. However, the actual species that gives rise to inhibition in a clinical setting has not been established. Recent studies by our group, using Raman microscopy and X-ray crystallography, have found that large quantities of enamine-based acyl-enzyme species are present within minutes in single crystals of SHV-1 β-lactamases which can lead to significant inhibition. The enamines are formed by breakdown of the cyclic β-lactam structures with further transformations leading to imine formation and subsequent isomerization to *cis* and/or *trans* enamines. Another favored form of inhibition arises from attack on the imine by a second nucleophilic amino acid side chain, e.g., from serine 130, to form a cross-linked species in the active site that can degrade to an acrylate-like species irreversibly bound to the enzyme. Thus, the imine is at a branch point on the reaction pathway. Using sulbactam and 6,6-dideuterated sulbactam we follow these alternate paths in WT and E166A SHV-1 β-lactamase by means of Raman microscopic studies on single enzyme crystals. For the unlabeled sulbactam, the Raman data show the presence of an acrylate-like species, probably 3-serine acrylate, several hours after the reaction is started in the crystal. However, for the 6,6-dideutero analogue the acrylate signature appears on the time scale of minutes. The Raman signatures, principally an intense feature near 1530 cm^{-1}, are assigned based on quantum mechanical calculations on model compounds that mimic acrylate species in the active site. The different time scales observed for acrylate-like product formation are ascribed to different rates of reaction involving the imine intermediate. It is proposed that for the unsubstituted sulbactam the conversion from imine to enamine, which involves breaking a C−H bond, is aided by quantum mechanical tunneling. For the 6,6-dideutero-sulbactam the same step involves breaking a C−D bond, which has little or no assistance from tunneling. Consequently the conversion to enamines is slower, and a higher population of imine results, presenting the opportunity for the competing reaction with the second nucleophile, serine 130 being the prime candidate. The hydrolysis of the resulting cross-linked intermediate leads to the observed rapid buildup of the acrylate product in the Raman spectra from the dideutero analogue. The protocol used here, essentially running the reactions with the two forms of sulbactam in parallel, provides an element of control and enables us to conclude that, for the unsubstituted sulbactam, the formation of the cross-linked intermediate and the final irreversible acrylate product is not a significant route to inhibition of SHV-1.

The issue of inhibitor resistance in class A β-lactamase is currently of paramount importance in clinical practice (*1*).

* To whom correspondence should be addressed. Department of Biochemistry, Case Western Reserve University, 10900 Euclid Avenue, Cleveland, OH 44106. Tel: (216) 368 0031. Fax: (216) 368 3419. E-mail: prc5@case.edu.

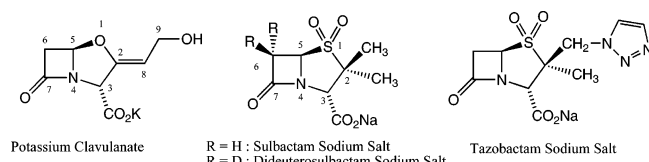[‡] Department of Biochemistry, Case Western Reserve University.
[§] Department of Chemistry, Case Western Reserve University.
[‖] Louis Stokes Cleveland Veterans Affairs Medical Center.
[⊥] Department of Medicine, Case Western Reserve University.
[#] Southern Methodist University.
[∇] Department of Pharmacology, Case Western Reserve University.

So far, the inhibitors used in clinical practice are specific for class A β-lactamases. They can be separated into two categories, sulfone inhibitors (sulbactam and tazobactam) and the non-sulfone inhibitor, clavulanic acid (Figure 1). The first step in the reaction pathway of a class A β-lactamase inhibitor with a β-lactamase is the formation of a Michaelis-type complex in the active site. This is followed by a nucleophilic attack at the lactam carbonyl by a serine side chain. In the resultant acyl-enzyme, a series of electron transfers occur, resulting in the opening of the thiazolium ring for tazobactam or sulbactam. A reactive imine (Scheme 1, species **2**) is formed that can undergo a number of transformations. The most likely process is hydrolysis of the imine, leading to free enzyme and a reaction product that

FIGURE 1: Class A β-lactamase inhibitors.

may further dissociate to a malonyl semialdehyde, and a second product. This dissociation may also occur prior to the hydrolysis step (2).

A second pathway is the formation of a transiently inhibited enzyme in which the imine acyl-enzyme tautomerizes to yield the more stable *cis*- or *trans*-enamine-based (species **3**, **4** in Scheme 1) structures. The third possible pathway is the attack by a second nucleophile, Ser130 in the class A TEM-1 and SHV-1 enzymes, at the C5 position of the reactive imine acyl-enzyme, leading to β-elimination across the C5−C6 bond and the formation of species **5** in Scheme 1. Further, a hydrolysis step occurs with the formation of a 5-atom vinyl carboxylic acid moiety attached to the second nucleophile (species **6** in Scheme 1) (3). The covalent modification of Ser130 leads to irreversible inhibition of the enzyme and has been previously observed by methods such as UV spectroscopy (4), mass spectrometry (5, 6), and X-ray crystallography (7, 8).

Despite these remarkable efforts it is still unclear whether transiently inhibited enzyme (species **2**−**4**) is the species that is responsible for the clinical utility of these compounds, or whether irreversible inhibition is required (species **5**, **6**). The present work addresses this issue and provides evidence that for sulbactam the irreversible inhibition products are formed inside a single crystal on a time scale that is longer than the bacterial half-life of 20−30 min. This indicates that transient inhibition may be responsible for the clinical utility of these compounds, since the formation of a transient enamine intermediate does occur within the 30 min time frame of the bacterial life cycle.

In our previous work, we have shown that the tracking and characterization of intermediates in SHV β-lactamase crystals can be accomplished using the interplay of two techniques, X-ray and Raman crystallography (9−12). These efforts were aided by using a deacylation deficient variant of the SHV-1 enzyme, E166A. We have shown that in the crystal structures for the clinically used mechanism-based inhibitors bound to the E166A variant of SHV-1 β-lactamase, a *trans*-enamine intermediate is formed, an indication that all of these inhibitors may follow a common pathway to inhibition (10, 11). In the present work we show that with sulbactam the wild-type SHV-1 β-lactamase forms a *trans*-enamine species, as well, within the time frame of 20−30 min. Sulbactam has been previously described not only as an inhibitor but also as a substrate of class A β-lactamases (2). Its analogue 6,6-dideuterated sulbactam (Figure 1) was shown to accelerate the hydrolysis and enzyme inactivation reactions with RTEM β-lactamase, a member of class A β-lactamase (2). Brenner and Knowles observed a 3-fold acceleration of both processes that was attributed to an inverse isotope effect, where processes involving the deuterated compounds proceeded more quickly. Their results were revolutionary at the time, but they did not provide a viable explanation for the identity of the product formed by

the 6,6-dideuterated sulbactam. In order to identify the product formed by a class A β-lactamase enzyme with 6,6-dideuterated sulbactam, we have performed Raman crystallography experiments on single crystals of the SHV-1 β-lactamase and its deacylation deficient E166A variant. Raman studies identified an α,β unsaturated product present in E166A β-lactamase after reacting with 6,6-dideuterated sulbactam and show that it is formed much more rapidly than the corresponding product from unsubstituted sulbactam.

MATERIALS AND METHODS

Inhibitors. Sulbactam was a generous gift of Pfizer. The sodium salt of 6,6-(dideutero)penicillanic acid sulfone was prepared from 6,6-dibromopenicillanic acid as described in the Supporting Information. Stock solutions at various concentrations in 2 mM HEPES buffer, pH 7.0 were prepared for use with the protein crystals.
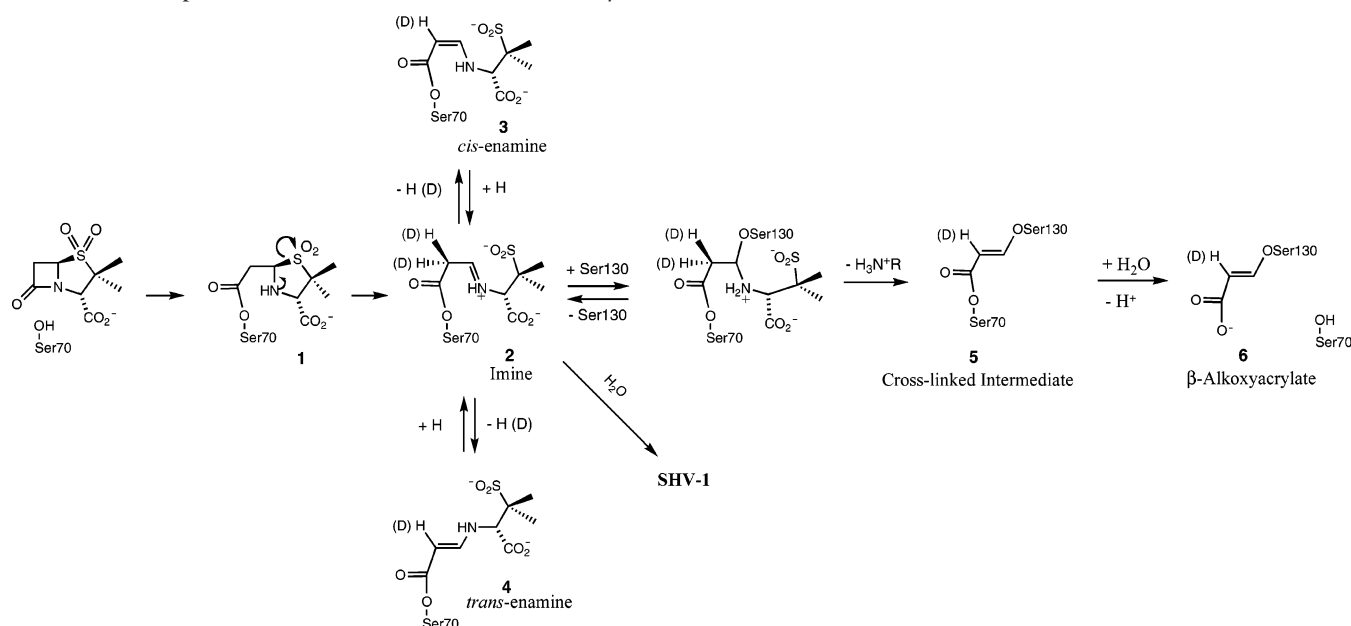
Protein Isolation and Purification. The wild-type SHV-1 β-lactamase was produced, isolated, and purified as previously described (13, 14). The E166A SHV clone was generated by site specific mutagenesis (14), and the protein was produced, isolated, and purified as previously described (13, 14). An additional HPLC[1] purification step was performed using a Sephadex Hi Load 26/60 column (Pharmacia, Uppsala, Sweden) and elution with phosphate buffered saline, pH 7.4.

Crystallization. All the proteins were concentrated to 5 mg/mL in 2 mM HEPES buffer, pH 7.0 for crystallization per the protocol of Kuzin et al. (15). Crystals in a 2 μL drop of mother liquor solution, typically $300 \times 300 \times 300$ μm in size, were transferred to a siliconized glass coverslip and washed 4 times with 0.1 M HEPES pH 7.0 to remove excess PEG-6000 prior to use with the Raman microscope. The WT and E166A forms of SHV-1 β-lactamase both crystallized in the $P2_12_12_1$ space group, and similar sized crystals, typically 100 μm in minimum dimension, were used for Raman crystallography.

Raman Crystallography. The Raman microscope system has been described previously (16, 17). The Raman spectra were excited with 100 mW of 647.1 nm irradiation at the crystal. After calibration peak positions are accurate to ± 1 cm^{-1}. During data collection, spectra were acquired over 10 s intervals and 10 spectra were averaged for each acquisition time point. Spectra of the apo-β-lactamase protein crystals were obtained, followed by addition of the inhibitors to the drop to achieve a final drop volume of 4 μL and different final inhibitor concentrations for certain experiments. Spectra were then acquired serially every 2−3 min following addition of inhibitor. Data collection and subtractions were performed using HoloGRAMS and GRAMS/AI 7 software (ThermoGalactic, Inc., Salem, NH). Raman spectra of the inhibitors used were obtained under like conditions. Spectra were obtained of 4 μL drops of inhibitor solutions prepared in 2 mM HEPES pH 7.0 at varying inhibitor concentrations.

Calculations. Ab initio quantum mechanical calculations were performed to predict the Raman spectra of compounds that model putative intermediate species using Gaussian 03

---

[1] Abbreviations: WT, wild-type; HPLC, high-pressure liquid chromatography; DFT, density functional theory.

Scheme 1.   Simplified Reaction Mechanism for Class A β-Lactamase with Sulbactam

RESULTS AND DISCUSSION

Sulbactam, Tazobactam, and Clavulanic Acid Form Large Populations of trans-Enamine Species with E166A β-Lactamase. The Raman spectra of the *trans*-enamine species formed by sulbactam, tazobactam, and clavulanic acid with E166A SHV-1 β-lactamase are discussed in Helfand et al. (*9*). These studies permitted us to identify the conditions needed for optimizing the *trans*-enamine populations in single crystals for flash freezing and subsequent X-ray crystallographic analysis. The maximum amount of the *trans*-enamine intermediate for all three inhibitors is attained within 20−30 min, a time frame relevant to bacterial half-lives. The structures of the intermediates from tazobactam, sulbactam, and clavulanic acid are presented in Padayatii et al. (*10, 11*). Some of the pertinent spectroscopic and structural findings are as follows:

(1) All three inhibitors formed single *trans*-enamine populations in the active site of E166A SHV-1 β-lactamase in single crystals within 30 min.

(2) Under "soak in" conditions of 5 mM ligand, tazobactam had an active site occupancy of 100% after about 10 min, whereas sulbactam and clavulanic acid had occupancies of 48% and 64%, respectively. However, by using higher concentrations of both ligands, approximatively 100% occupancy could be achieved for X-ray analysis.

(3) The most intense *trans*-enamine Raman feature occurs near 1595 cm^{-1} for all three inhibitors. Small differences in the position may reflect small differences in the *trans*-enamine skeleton. Thus, the most planar *trans*-enamine formed by clavulanic acid has $\nu_{O=C-C=C-NH-}$ at 1612 cm^{-1}, whereas the intermediate from tazobactam has a C−C=C−N dihedral angle of 168° and this distortion can account, in part, for the symmetric stretch occurring at the lower frequency of 1593 cm^{-1}.

After Several Hours There Is Evidence for Significant Populations of an Acrylate-like Species. In order to elucidate the intermediates formed in a single crystal of the E166A variant of SHV-1 β-lactamase with sulbactam on a longer time scale, a 30 h long experiment was undertaken, and the Raman difference spectra of sulbactam reacting in the enzyme at different time points are shown in Figure 2. Part of the rationale for this is that long soak times were used for the structure determination of tazobactam reacting inside a wild-type SHV-1 β-lactamase (*8*). Figure 2 presents in the top panel the Raman difference spectrum of sulbactam reacting inside the E166A variant of SHV-1 β-lactamase after 20 min. This result was discussed in the previous section, where a *trans*-enamine species is identified in the active site, with a Raman signature peak at 1598 cm^{-1}.

The middle and lower panels of Figure 2 identify a new peak at 1530 cm^{-1} that increases in intensity with time. The time dependence is shown in Figure 3 over the 30 h experiment.

Traces of the 635 cm^{-1} feature given by the thiazolium ring are still present, which suggests the possibility of some acyl-enzyme (species **1** in Scheme 1) or unreacted sulbactam being present. Based on quantum mechanical calculations, the fragment giving rise to the 1530 cm^{-1} band was identified as species **6** in Scheme 1, a 3 serine acrylate. The compound used to model species **6** is shown in Figure 4, where serine is replaced by a methyl group. In the calculated spectrum, Figure 4, the major feature is the 1536 cm^{-1} peak, which corresponds to the 1530 cm^{-1} experimental value. The mode is given mostly by C=C stretching and delocalized motions over the whole acrylate chain and is the most intense feature of the spectrum. The calculated feature at 1628 cm^{-1} is assigned to coupled C=O and C=C motions, but is not observed in the experimental Raman difference spectrum due to the difficulties in detecting anything in the 1650 cm^{-1} region, where the intense amide I peak of the protein "swamps" other features and impedes accurate spectral subtractions. Also, the calculated feature at 1330 cm^{-1} corresponds to the experimental band near 1300 cm^{-1} and
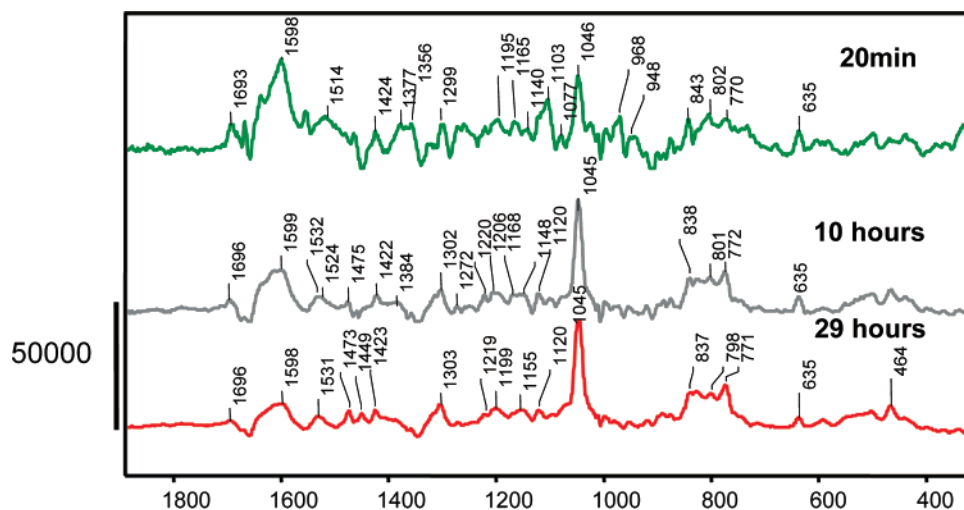
FIGURE 2: Raman difference spectra of E166A SHV-1 *β*-lactamase reacting with sulbactam 5 mM at different time points. The peak near 1045 cm^{-1} is due to HEPES buffer.
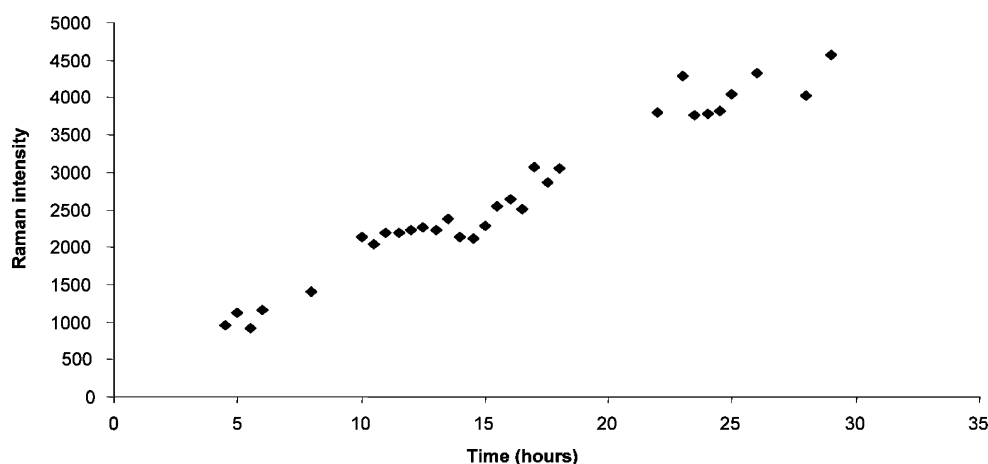

FIGURE 3: Time dependence of the 1530 cm^{-1} feature height given by sulbactam reacting inside an E166A SHV-1 *β*-lactamase crystal. The estimated standard deviation in the intensity values is ±12%.

is assigned mostly to C=C stretching coupled to C−H bending.

Calculations were also undertaken for the Raman spectrum of the methyl 3-methoxy acrylate which models species **5** in Scheme 1. The model compound has an intense band at 1707 cm^{-1} given by the C=O stretch and C−H wag (Figure 2 Supporting Information), while the C=C stretching and delocalized motion over the entire chain is present at 1567 cm^{-1}. Since in the experimental spectra no feature at 1707 cm^{-1} can be identified and the main C=C stretching frequency occurs at 1530 cm^{-1}, the methyl 3-methoxy acrylate (species **5**, Scheme 1) is not the prime candidate for the intermediate formed by the sulbactam or 6,6-dideuterated sulbactam in the E166A variant of SHV-1 *β*-lactamase, see below. Even if the methyl 3-methoxy acrylate would be present in the active site in a strained conformation that would accommodate this shift in the C=C stretching motion, the C=O stretching feature cannot be accounted for. In conclusion, the 3-methoxy acrylate (species **6** in Scheme 1) was identified as the product present in the active site of E166A with sulbactam and 6,6-dideuterated sulbactam giving rise to a feature near 1530 cm^{-1}.

The time dependence of the 1530 cm^{-1} feature is shown in Figure 3, where the intensity of the acrylate peak was plotted as a function of time. There is no steady state attained

and the acrylate population seems to increase continuously over the 30 h period. Times longer than 30 h could not be probed due to crystal instability. What is remarkable is that the acrylate species takes hours to emerge in the E166A variant with sulbactam, as opposed to the *trans*-enamine that reaches a maximum within 30 min. This leads us to conclude that the *trans*-enamine intermediate is important for inhibition, while the acrylate is a species that is formed too late in time to be relevant to affect the bacterial life cycle.

6,6-Dideuterated Sulbactam Forms the Acrylate Species with E166A SHV-1 β-Lactamase in Minutes. As mentioned above, Brenner and Knowles were able to observe an acceleration of the reaction of 6,6-dideuterated sulbactam with a similar class A, RTEM *β*-lactamase (*2*). In order to identify whether this applies to SHV as well, Raman crystallography was used to monitor the reaction of the E166A variant of SHV-1 *β*-lactamase with 6,6-dideuterated sulbactam, and the Raman difference spectra at different time points are shown in Figure 5. For the unlabeled sulbactam reacting with the E166A variant an enamine was observed at 20 min (Figure 2); however, in the case of the 6,6-dideuterated sulbactam at 20 min, a mixture of the enamine at 1591 cm^{-1} and the acrylate form at 1531 cm^{-1} is observed. The latter feature increases in intensity with time, see middle and lower panels of Figure 5. The experimental downshift
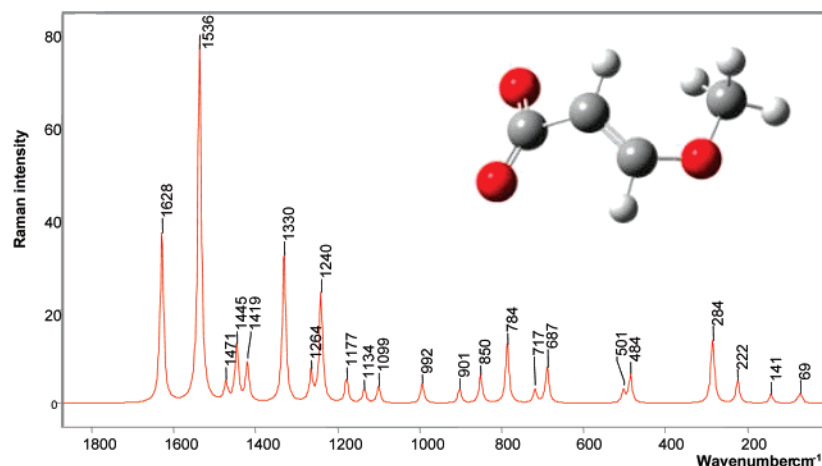
Calculated Raman v/cm⁻¹ for CH3OCHCHCOO⁻/ CH3OCHCDCOO⁻ intensities are shown in parenthesis	Assignment
1628 (37)/1627 (34)	CH wagging and COO⁻ anti-symmetric stretching
1536 (80)/1513(92)	C=C, COO⁻ stretching, delocalized stretching over the entire chain
1330(32)	CH₃, CH wagging, delocalized stretching over the entire chain
1240 (24)/1235(30)	CH wagging, COO⁻ stretching

FIGURE 4: Calculated Raman spectrum of 3-methoxyacrylate, obtained by using the Gaussian 03 software, where the main features are 1629 cm⁻¹ C=O and C=C stretch, 1536 cm⁻¹ C=C stretch and delocalized motions over the entire chain, 1330 cm⁻¹ C=C stretch and C−H bending, 1240 cm⁻¹ C=C and C=O stretch, C−H bending.
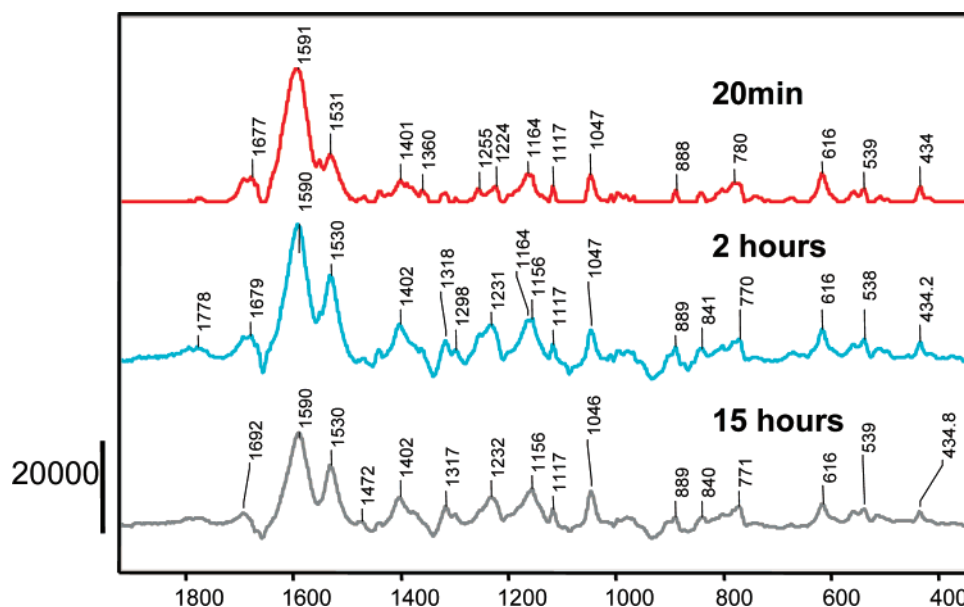

FIGURE 5: Raman difference spectra of E166A SHV-1 β-lactamase reacting with 6,6-dideuterated sulbactam 10 mM at different time points.

of the wavenumber of the enamine for the deuterated compound, compared to unlabeled sulbactam, 1591 versus 1598 cm⁻¹ (Figures 2 and 5), is reproduced by quantum mechanical calculations that suggest a downshift of 10 cm⁻¹. However, for the acrylate band near 1530 cm⁻¹ there appears to be little or no shift for the species emanating from 6,6-dideuterated sulbactam. However, calculations indicate that a shift of ∼20 cm⁻¹ should occur (Figure 4), upon deuterium substitution. This suggests that the C−D, C−H exchange has occurred prior to acrylate formation, consistent with the

observation of Brenner and Knowles (2) that both protons at C6 exchange with the D₂O solvent during the reaction. However, the details of the chemistry of these exchanges have not been elucidated. Traces of the 616 cm⁻¹ feature given by the thiazolium ring (Figure 1, Supporting Information) are still observed. The 1047 cm⁻¹ peak is given by an incomplete subtraction of a HEPES buffer feature.

The 1530 cm⁻¹ feature appears much more quickly compared to unsubstituted sulbactam (Figure 6). This can be explained by the fact that the transformation step of the
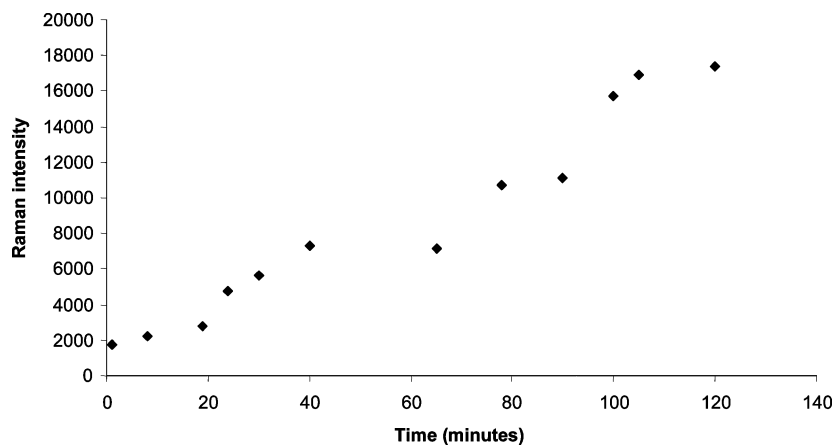
FIGURE 6: Time dependence of the 1530 cm^{-1} feature height given by 6,6-dideuterated sulbactam reacting inside an E166A SHV-1 β-lactamase crystal. The estimated standard deviation in the intensity values is $\pm12\%$.
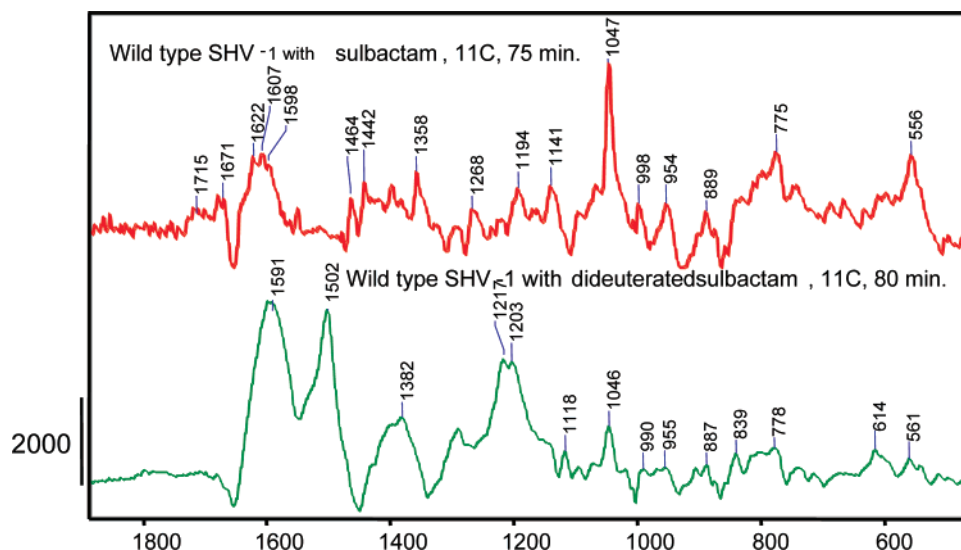

FIGURE 7: Raman difference spectra of wild-type SHV-1 β-lactamase reacting with sulbactam (red) at 75 min or 6,6-dideuterated sulbactam (green) at 80 min.

imine to an enamine in Scheme 1 is isotopically sensitive. This transformation requires the breaking of a C−D bond for the deuterated compound, as opposed to a C−H bond for sulbactam. It is postulated that the imine to enamine reaction for unsubstituted sulbactam is assisted by quantum mechanical tunneling, favoring this pathway, while this mechanism is unavailable for the deuterated sulbactam resulting in retardation of C−D compared to C−H bond breaking (*19*). This subsequently leads to a greater accumulation of the imine in the deuterated compared to the unsubstituted compound. The imine is not detected in the Raman data since it has a lower scattering section than the enamine and acrylate species. The imine can undergo either a hydrolysis or a second nucleophilic attack from serine 130 (Scheme 1) leading to a cross-link (species **5** in Scheme 1). Hence higher populations of the species **5** and **6** in Scheme 1 are attained rapidly for the deuterated species. The time dependence of the acrylate species formed by the 6,6-dideuterated sulbactam is shown in Figure 6, where the 1530 cm^{-1} feature is observable immediately and significantly higher amounts of the product are produced in a much shorter time frame, compared to unsubstituted sulbactam. Thus, at 2 h the 6,6-dideuterated sulbactam forms a product peak with 18000 standard intensity units, while the unlabeled
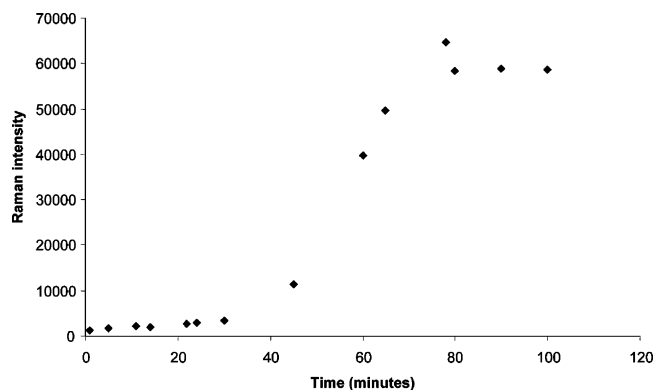

FIGURE 8: Time dependence of the 1502 cm^{-1} feature height given by 6,6-dideuterated sulbactam reacting inside a WT SHV-1 β-lactamase crystal. The estimated standard deviation in the intensity values is $\pm12\%$.

compound forms a feature of 4500 standard intensity units at 29 h.

No Evidence for Acrylate Species in the Reaction of Wild-Type SHV-1 with Sulbactam, While 6,6-Dideuterated Sulbactam Does Form a Large Population of Acrylate Species. The reaction of WT SHV-1 β-lactamase with 6,6-dideuterated sulbactam (15 mM) also reveals the presence of a 3 serine acrylate in the active site. This is evidenced by the

intense feature at 1502 cm^{-1} in the lower panel in Figure 7. The putative acrylate feature shows a downshift, compared to the E166A variant which occurred at 1530 cm^{-1}, which is ascribed to the effects of electron polarization in the active site of the WT enzyme. It has been known for some time that charged groups or dipoles near an α,β unsaturated ligand can polarize the π electrons giving rise to up to 50 cm^{-1} downshift in the frequency of the delocalized C=C stretching mode (*20*). Similar effects may be occurring, polarizing the acrylate π electrons in WT β-lactamase, but in the absence of X-ray data for the product complex the details are not known. The 6,6-dideuterated sulbactam appears to reach a steady state for the α,β unsaturated product around 80 min, as shown in Figure 8 (the difference in kinetic profiles in Figures 6 and 8 is due to the fact that E166A plays a role in acylation). Also, in the lower trace in Figure 7 an enamine feature (1591 cm^{-1}) can be detected in a similar position to the one observed for the E166A variant of SHV-1 β-lactamase reacting with the deuterated compound, 1590 cm^{-1} (Figure 5). In contrast to the results for the deuterated compound, the Raman difference spectrum of unsubstituted sulbactam reacting with WT SHV-1 β-lactamase does not show any evidence of a band in the 1500 cm^{-1} region due to a 3 methoxy acrylate at 75 min (Figure 7, top trace). Moreover, there is no evidence for a band near 1500 cm^{-1} for sulbactam reacting with WT SHV-1 β-lactamase at 24 h (data not shown), whereas for the E166A variant of SHV-1 β-lactamase the 1530 cm^{-1} can be detected (Figure 2). Taken together the data indicate that the 6,6-dideuterated sulbactam leads to an acceleration of the production of the 3 methoxy acrylate species, compared to the unlabeled compound in both wild-type and E166A SHV-1 β-lactamase.

CONCLUSION

We were able to follow the reaction between sulbactam and E166A or WT SHV-1 β-lactamase in single crystals by using a Raman microscope. The use of 6,6-dideuterated sulbactam allows us to compare two reaction pathways stemming from the imine intermediate (species **2**, Scheme 1). For both forms of the enzyme with 6,6-dideuterated sulbactam there is evidence for the formation of a 3-serine acrylate species within 20 min. This species is formed by the imine being attacked by a second nucleophile, proposed to be Ser130. Subsequent hydrolysis of the product cross-linking Ser70 and Ser130 yields the 3-serine acrylate. However, while the unsubstituted sulbactam quickly yields a *trans*-enamine population derived from the imine, it takes several hours before a 3-serine acrylate species can be detected. This leads us to conclude that in the normal reactions of sulbactam with the SHV-1 enzyme irreversible inhibition via 3-serine acrylate plays little or no role in inhibition on the time scale compatible with bacterial half-life of 20−30 min.

SUPPORTING INFORMATION AVAILABLE

(1) Raman spectrum of 6,6-dideuteropencillanic acid sulfone, (2) calculated Raman spectra of methyl 3-methoxy-acrylate and 2, deutero methyl 3-methoxyacrylate, and (3) synthesis of 6,6-dideuteropencillanic acid sulfone. This material is available free of charge via the Internet at http://pubs.acs.org.

REFERENCES

1. Helfand, M., and Bonomo, R. (2003) β-Lactamases: A Survey of Protein Diversity, *Curr. Drug Targets 3*, 9−23.
2. Brenner, D. G., and Knowles, J. R. (1981) Penicillanic Acid Sulfone: An Unexpected Isotope Effect in the Interaction of 6a- and 6b-Monodeuterio and of 6,6-Dideuterio Derivatives with RTEM β-Lactamase from Escherichia coli, *Biochemistry 20*, 3680−3687.
3. Bonomo, R. A., Dawes, C. G., Knox, J. R., and Shlaes, D. M. (1995) β-Lactamase mutations far from the active site influence inhibitor binding, *Biochim. Biophys. Acta 1247*, 121−125.
4. Bush, K., Clarissa, M., Rasmussen, B. A., Lee, V. J., and Yang, Y. (1993) Kinetic Interactions of Tazobactam with β-Lactamases from All Major Structural Classes, *Antimicrob. Agents Chemother. 37*, 851−858.
5. Brown, R. P. A., Aplin, R. T., and Schofield, C. J. (1996) Inhibition of TEM-2 β-Lactamase from Escherichia coli by Clavulanic Acid: Observation of Intermediates by Electrospray Ionization Mass Spectrometry, *Biochemistry 35*, 12421−12432.
6. Yang, Y., Janota, K., Tabei, K., Huang, N., Siegel, M. M., Lin, Y.-I., Rasmussen, B. A., and Shlaes, D. M. (2000) Mechanism of Inhibition of the Class A b-Lactamases PCI and TEM-1 by Tazobactam: Observation of Reaction Products by Electrospray Ionization Mass Spectrometry, *J. Biol. Chem. 275*, 26674−26682.
7. Chen, C. C. H., and Herzberg, O. (1992) Inhibition of β-lactamase by clavulanate: Trapped intermediates in cryocrystallographic studies, *J. Mol. Biol. 224*, 1103−1113.
8. Kuzin, A. P., Nukaga, M., Nukaga, Y., Hujer, A., Bonomo, R. A., and Knox, J. R. (2001) Inhibition of the SHV-1 beta-Lactamase by Sulfones: Crystallographic Observation of Two Reaction Intermediates with Tazobactam, *Biochemistry 40*, 1861−1866.
9. Helfand, M. S., Totir, M. A., Carey, M. P., Hujer, A. M., Bonomo, R. A., and Carey, P. R. (2003) Following the Reactions of Mechanism-Based Inhibitors with β-Lactamase by Raman Crystallography, *Biochemistry 42*, 13386−13392.
10. Padayatti, P. S., Helfand, M. S., Totir, M. A., Carey, M. P., Carey, P. R., Bonomo, R. A., and van den Akker, F. (2005) High Resolution Crystal Structures of the trans-Enamine Intermediates Formed by Sulbactam and Clavulanic Acid and E166A SHV-1 {beta}-Lactamase, *J. Biol. Chem. 280*, 34900−34907.
11. Padayatti, P. S., Helfand, M. S., Totir, M. A., Carey, M. P., Hujer, A. M., Carey, P. R., Bonomo, R. A., and Akker, F. v. d. (2004) Tazobactam Forms a Stoichiometric trans-Enamine Intermediate in the E166A Variant of SHV-1 β-Lactamase: 1.63 Å Crystal Structure, *Biochemistry 43*, 843−848.
12. Totir, M. A., Padayatti, P. S., Helfand, M. S., Carey, M. P., Bonomo, R. A., Carey, P. R., and Akker, F. v. d. (2006) Effect of the Inhibitor-Resistant M69V Substitution on the Structures and Populations of trans-Enamine beta-Lactamase Intermediates, *Biochemistry 45*, 11895−11904.
13. Helfand, M. S., Hujer, A. M., Sonnichsen, F. D., and Bonomo, R. A. (2002) Unexpected Advanced Generation Cephalosporinase Activity of the Met69Phe Variant of SHV β-Lactamase, *J. Biol. Chem. 277*, 47719−47723.
14. Hujer, A. M., Hujer, K. M., and Bonomo, R. A. (2001) Mutagenesis of amino acid residues in the SHV-1 β-lactamase: the premier role of Gly238Ser in penicillin and cephalosporin resistance, *Biochim. Biophys. Acta 1547*, 37−50.
15. Kuzin, A. P., Nukaga, M., Nukaga, Y., Hujer, A. M., Bonomo, R. A., and Knox, J. R. (1999) Structure of the SHV-1 beta-lactamase, *Biochemistry 38*, 5720−5727.
16. Altose, M. D., Zheng, Y., Dong, J., Palfey, B. A., and Carey, P. R. (2001) Comparing protein-ligand interactions in solution and single crystals by Raman spectroscopy, *Proc. Natl. Acad. Sci. U.S.A. 98*, 3006−3011.
17. Dong, J., Swift, K., Matayoshi, E., Nienaber, V. L., Weitzberg, M., Rockway, T., and Carey, P. R. (2001) Probing Inhibitors Binding to Human Urokinase Crystals by Raman Microscopy: Implications for Compound Screening, *Biochemistry 40*, 9751−9757.
18. Frisch, M. J., Trucks, G. W., Schlegel, H. B., Scuseria, G. E., Robb, M. A., Cheeseman, J. R., Montgomery, J. A., Jr., Vreven, T., Kudin, K. N., Burant, J. C., Millam, J. M., Iyengar, S. S., Tomasi, J., Barone, V., Mennucci, B., Cossi, M., Scalmani, G.,

Rega, N., Petersson, G. A., Nakatsuji, H., Hada, M., Ehara, M., Toyota, K., Fukuda, R., Hasegawa, J., Ishida, M., Nakajima, T., Honda, Y., Kitao, O., Nakai, H., Klene, M., Li, X., Knox, J. E., Hratchian, H. P., Cross, J. B., Bakken, V., Adamo, C., Jaramillo, J., Gomperts, R., Stratmann, R. E., Yazyev, O., Austin, A. J., Cammi, R., Pomelli, C., Ochterski, J. W., Ayala, P. Y., Morokuma, K., Voth, G. A., Salvador, P., Dannenberg, J. J., Zakrzewski, V. G., Dapprich, S., Daniels, A. D., Strain, M. C., Farkas, O., Malick, D. K., Rabuck, A. D., Raghavachari, K., Foresman, J. B., Ortiz, J. V., Cui, Q., Baboul, A. G., Clifford, S., Cioslowski, J., Stefanov, B. B., Liu, G., Liashenko, A., Piskorz, P., Komaromi, I., Martin, R. L., Fox, D. J., Keith, T., Al-Laham, M. A., Peng, C. Y., Nanayakkara, A., Challacombe, M., Gill, P. M. W., Johnson, B., Chen, W., Wong, M. W., Gonzalez, C., and Pople, J. A. (2004) *Gaussian 03*, revision C.02, Gaussian, Inc., Wallingford, CT.

19. Nagel, Z. D., and Klinman, J. P. (2006) Tunneling and Dynamics in Enzymatic Hydride Transfer, *Chem. Rev. 106*, 3095−3118.

20. Carey, P. R. (2006) Spectroscopic Characterization of Distortion in Enzyme Complexes, *Chem. Rev. 106*, 3043−3054.